Proceedings of the 4th International Conference on Biological Engineering and Medical Science
DOI: 10.54254/2753-8818/73/2024.19379

Low-density Lipoprotein as an Endogenous Cancer-Targeting Carrier for Cholesterol-Drug Delivery: A Molecular Dynamics Simulation Study

Zishuo Li

Keystone Academy, Beijing, China

lizishuo703100@gmail.com

Abstract. Despite systematically targeting rapidly proliferating cells and resulting in effective cell death, conventional chemotherapy is subject to the limitation of non-specificity in terms of delivery to cancer cells. Hydrophilic chemotherapeutic drugs are further hampered by a short half-life due to rapid clearance. A promising new approach to address the issues with chemotherapy is exploiting endogenous low-density lipoprotein (LDL) for anticancer drug delivery. These non-immunogenic and intrinsically stable nanoparticles interact with LDL receptors, which are often overexpressed by a wide range of cancer cells. As a result, many therapeutic agents can be loaded into LDL's hydrophobic core and directed to cancer cells via the specific LDL-LDLR interaction. Here we report the strategy of conjugating cholesterol to a hydrophilic antimetabolite chemotherapy drug, gemcitabine, in an attempt to facilitate its partition into the hydrophobic core of LDL and hence targeted drug delivery. The results of the molecular dynamics simulation show that the cholesterol-gemcitabine bioconjugate partitioned deeper into the LDL with a greater decrease in free energy compared to the original drug, validating the general strategy of conjugating cholesterol with chemotherapy drugs for LDL delivery.

Keywords: Low-density Lipoprotein, Chemotherapy, Drug Delivery, Cholesterol Conjugation, Gemcitabine, Molecular Dynamics Simulation, Cancer.

1. Introduction

Cancer has been a major public health problem globally, affecting millions of people and causing significant morbidity and mortality. According to the World Health Organization (WHO), cancer is the second-leading cause of death worldwide, accounting for an estimated 609,820 million deaths in the U.S. in 2023, which corresponds to 1670 deaths per day [1]. Cancers of the breast, lung, colon and rectum, prostate, skin, and stomach are the most frequently diagnosed on a global scale. [2]. Lung cancer remains the leading cause of cancer worldwide, resulting in approximately 350 deaths each day in the U.S. [3]. Conventional cancer therapies include surgical excision, irradiation, and chemotherapy. The surgical approach involves physically removing the solid tumor from a certain area in the patient's body, commonly performed on breast cancer, pancreatic cancer, and so forth [4]. The irradiation approach, or radiotherapy, uses high doses of radiation to kill cancer cells, slow their growth through DNA damage, and shrink tumors in areas such as the head and neck, breast, cervix, and so on. Local treatments, surgical excision, and irradiation therapy are most suited to solid tumors contained in one area [5]. Chemotherapy,

© 2025 The Authors. This is an open access article distributed under the terms of the Creative Commons Attribution License 4.0 (https://creativecommons.org/licenses/by/4.0/).

DOI: 10.54254/2753-8818/73/2024.19379

on the other hand, is a more systematic treatment that targets all rapidly proliferating cells throughout the body [6]. Utilizing the circulation of drug molecules through the bloodstream, chemotherapy exhibits its advantage in reaching not only the primary tumor but any metastatic cancer cells in other tissues that are difficult to locate precisely [7]. After oral or intravenous administration, the potent chemotherapy drugs interfere with the cancer cells' rapid division and proliferation, ultimately leading to cell death [8]. It is now common medical practice to adopt chemotherapy in conjunction with other modalities, such as surgery and radiotherapy, in cancer treatments [9].

However, despite its capability to target all cancer cells systematically and its effectiveness in resulting cell death, chemotherapy is challenged by a range of limitations. Primarily, the non-specificity of chemotherapy accounts for its non-selective targeting of both cancer cells and rapidly proliferating normal cells, such as those in the bone marrow, gastrointestinal tract, and hair follicles [10]. In the long term, this can lead to an array of side effects that significantly impact patients' life quality, including hair loss, nausea, vomiting, fatigue, and increased susceptibility to infections [11]. In addition, many hydrophilic chemotherapy drugs are subject to rapid clearance after administration. Due to their high hydrophilicity, these drug molecules tend to dissolve readily in an aqueous environment and, as a result, can be filtered by the kidneys and excreted in the urine relatively quickly [12]. Metabolism can also help to facilitate the rapid clearance of hydrophilic drugs from the systemic circulation. As a result, hydrophilic drugs suffer from a shorter half-life and reduced systemic exposure compared to more hydrophobic drugs, compromising their ability to achieve therapeutic concentration and sufficient duration [13]. For certain sensitive tumors, standard chemotherapy can be effective in the beginning but gradually fail in the course of treatment due to multidrug resistance (MDR), which is a further limitation [10].

To improve the efficacy of chemotherapy in cancer treatment, it is of utter importance to enhance the drug molecules' specificity in targeting cancer cells and their stability in bloodstream circulation for a prolonged effect. A promising new method to address the limitations of chemotherapy is exploiting endogenous lipoproteins (LPs) for anticancer drug delivery [14]. LPs are heterogeneous nanoparticles produced by the liver and intestines [15]. Having a generally spherical shape, they facilitate the complex metabolism of lipids by transporting them from the intestines to other tissues for storage or from tissues to the liver for catabolism. Due to their biogenic, intrinsically stable, and non-immunogenic nature, LPs have been described as effective carriers for targeted delivery of various drugs [14]. LPs cover a wide range of sizes and densities with different lipid-protein ratios; low-density lipoproteins (LDLs) draw special attention due to their ability to interact with specific cell types involved in lipid metabolism by binding to specific receptors, such as the LDL receptor (LDL-R) [16]. Notably, LDL-R is frequently overexpressed in cancer cells; this abnormally high metabolic rate necessitates accelerated membrane biogenesis and higher biofunctional requirements that would not be possible without the increased uptake of cholesterol carried by LDLs [17]. LDL-based therapy can also target tumor-associated macrophages (TAMs) and monocytes in the tumor microenvironment, which promote tumor progression through high-level expressions of scavenger receptors that internalize modified LDL [18]. Therefore, using LDL as an endogenous anticancer drug carrier is a new possibility for the indirect targeting of cancer cells, utilizing their property of displaying high expression and activity of LDL-R, which is not observed in normal proliferating cells [19]. Aside from high specificity, LDLs also display desirable stability and safety when used in drug delivery. LDL, as a type of LP, has a similar structure and composition to synthetic liposomes. Nevertheless, in comparison with LDL, the latter has shorter circulation times unless coated with additional polyethylene glycol (PEG), which then increases the risk of activating the immune system after repeated administration. In contrast, LDLs naturally evade the immune system and hence allow for prolonged circulation times, eliminating the risk of clearance and potentially adverse effects on the body [14]. Longer circulation is desired, as it means increased interactions with targeted tissues.

With a broad array of advantages, LDLs are used to load many therapeutic agents, such as chemotherapy drugs, photosensitizers, nucleotides, HIV drugs, and imaging agents [20]. Here, we investigate the possibility of conjugating a hydrophilic antimetabolite chemotherapy drug, gemcitabine,

DOI: 10.54254/2753-8818/73/2024.19379

to cholesterol in order to facilitate its transfer into the hydrophobic core of LDL for targeted delivery to cancer cells. Previous studies have shown that the bioconjugation of squalene to hydrophilic drugs displays spontaneous, strong interaction with cholesterol-rich LDLs both in vitro and in vivo [16,21]. Since cholesterol is essentially a successor of squalene and they are similar in their hydrophobic nature, it is hypothesized that the bioconjugate of hydrophilic chemotherapy drugs and cholesterol by single covalent linkage will display preeminent affinity towards LDL and undergo spontaneous incorporation into the hydrophobic core of LDL [22-24]. Afterward, the circulation in the bloodstream is expected to precisely deliver the drug conjugate to cancer cells through the binding of LDL and LDL-R on cancer cells, leading to cellular uptake and effective targeting even during chemotherapy [23,25].

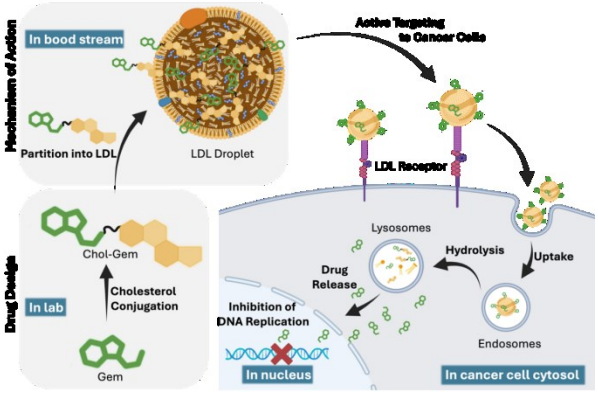


Figure 1. The schematic shows the strategy of cholesterol conjugation to Gemcitabine for enhanced partition into LDL particles and targeting of drug delivery to cancer cells.

As a proof of concept, the cholesterol-conjugated gemcitabine (CGem) was selected as the drug model in this study to investigate the LDL-targeting effect. Molecular dynamics (MD) simulations were performed to study the molecular interactions between LDL and Gem or CGem drugs [26]. From the conventional simulations, we found that CGem partitioned deeper into the LDL membrane model due to the enhanced hydrophobic interactions between the internal LDL core and the cholesterol tail of CGem. In contrast, Gem interacted favorably with the hydrophilic phospholipid heads of the LDL surface. Further calculation of the binding free energy revealed CGem's superior binding affinity to LDL. The results indicate that the cholesterol conjugation to Gem can promote the drug partition into LDL with a stronger binding affinity, potentially improving the pharmacodynamics of hydrophilic chemotherapeutic drugs and achieving cancer-targeted therapy via LDL (Figure 1). In principle, this strategy holds the promise that it is transferable and can be generalized to a class of hydrophilic small-molecule cancer therapeutics.

2. Methods

2.1. Implementation of Molecular Dynamics Simulations

In this study, the MD simulations were performed using GROMACS 2023.3. For the LDL compartment, the SLipids force field was used because it is one of the best all-atom force fields for describing lipids above their melting point [27,28]. The General Amber Force Field (GAFF) force field was chosen for small drug-like molecules due to its accuracy, wide parameter coverage, and benchmarked compatibility with SLipids [29-31]. For cholesteryl oleate components, the force field parameters of oleate were derived by GAFF, while those for the remaining cholesterol moiety were taken from the SLipids force field. The TIP3P water model was adopted for all the simulations [32]. All simulations were implemented in an NPT ensemble with a temperature of 310 K and a pressure of 1 bar, maintained by the v-rescale thermostat and c-rescale barostat, respectively [33]. A timestep of 1 fs was used, and the leap-frog integrator was used to integrate the atomic motions [34]. The cutoff distance for van der Waals

DOI: 10.54254/2753-8818/73/2024.19379

and electrostatic interactions was both set to 1.0 nm [35]. The particle mesh Ewald (PME) summation algorithm was utilized to compute the long-range electrostatic forces [36,37].

2.2. Parameterization of the Drug Molecules

To study the advantages of cholesterol conjugation to hydrophilic drugs, we designed two drugs, Gem and CGem, as the control and experiment models, respectively [38]. The only difference between the two is the cholesterol conjugation on CGem (Figure 2). The molecular structures were first drawn on ChemDraw 16 and then converted to 3D models by Marvin Sketch [39,40]. The subsequent atomic topologies were saved as mol2 files. Subsequently, the Acpype topology generator took these topology files and conducted force matching using the GAFF [41]. In addition, the charge of each atom was derived using the AM1-BCC scheme, which has been used and benchmarked in several studies [42]. The additional nonbonded parameters and atom types from GAFF were added to the SLipids force field.

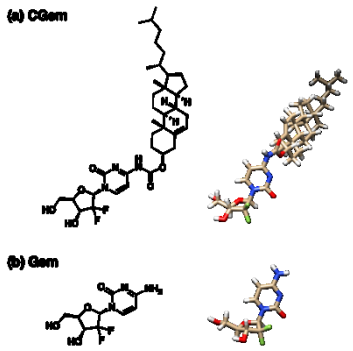


Figure 2. The chemical structures and the modeled structures of (a) CGem and (b) Gem. The 3D models were visualized by Chimera.

2.3. LDL Model Construction and Equilibration

LDLs are spherical particles, 22–29 nm in diameter, with a core of esterified cholesterol and triglyceride, a surface lipid coat of unesterified cholesterol and phospholipid, and apo B, an essential structural protein [43]. Since apo B is not the major event when studying the interactions between the drug molecule and the LDL internal core, we neglect the surface protein when establishing the LDL model. In addition, due to the large size of such compartments, simulating an entire LDL using all-atom simulations is intractable with our available computational resources. Thus, we reduce the LDL model to a symmetric bilayer membrane as shown in Figure 3. Essentially, a middle slice of the spherical LDL particle is taken and set up in a simulation box with periodic boundary conditions. This model consists of a hydrophobic core and lipid coating on each side, resembling the real LDL, and hence was suitable for our study. To further reduce the computational cost, we slightly decreased the dimension of the inner core along the X-axis.

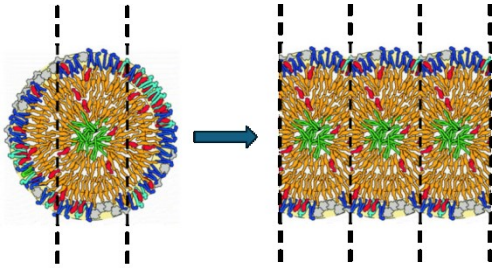


Figure 3. The scheme of reducing a spherical LDL particle into a thick bilayer membrane model in periodic boundary conditions for MD simulations.

DOI: 10.54254/2753-8818/73/2024.19379

Specifically, the LDL model alone was initially placed in a box with the x, y, and z dimensions being 5 nm, 5 nm, and 12 nm, respectively. A total of approximately 43,000 atoms were contained in the box. Each type of constituent molecule, including 1-palmitoyl-2-oleoyl-sn-glycero-3-phosphocholine (POPC), 1-palmitoyl-2-hydroxy-sn-glycero-3-phosphocholine (LysoPC), cholesterol (CHL), cholesteryl oleate (CO), and glyceryl trioleate (GO), is placed within the box corresponding to their respective ratio in a real LDL particle. Next, the simulation box was extended by 4.8 nm in the +Z direction and 2.8 nm in the -Z direction to accommodate water molecules, resulting in a final box of $5\times5\times19.6$ nm^3 (490 nm^3) in dimension. For subsequent free energy calculations, the thicker water layer in the +Z direction was set. Table 1 shows the number of each molecule in the LDL model. All components were packed into the simulation box by Packmol [44].

Table 1. The number of molecules in the LDL model

Molecule Type	Number
CO	90
GO	10
CHL	33
POPC	60
LyPC	8
Water	6500

The energy minimization was performed using the steepest descent algorithm, with a force tolerance of 1000 kJ/mol/nm. The system was subsequently equilibrated in the NVT ensemble for 10 ps, followed by the NPT ensemble for 100 ns. The equilibration was run under semi-isotropic pressure control for membrane systems, with the x and y directions of the model coupled while the z direction was separately controlled. To examine the equilibration of the LDL membrane model, the average partial density from the final 25 ns was extracted to visualize the distribution of each molecule. In addition, the temperature, pressure, and potential energy were shown to confirm that the system was well-equilibrated and suitable for subsequent modeling.

2.4. Interaction Between the Drug and LDL

To study the binding event of drug molecules to the LDL, we conducted long conventional MD simulations by inserting a drug in the upper water phase and allowing it to freely diffuse until forming a stable adduct with LDL. The upper water phase was thought to be the circulation environment. After the drug was bound to LDL, the Z positions and partial densities of the CGem and Gem were extracted from the trajectories to determine the depth of the insertion. The trajectories were also visualized to investigate the orientation of the drug molecules after binding to LDL.

2.5. Steered MD Simulations and Umbrella Sampling

To calculate the binding free energy, using an unbiased method would be intractable because it is impossible to sample the low-probability phase space, i.e., the dissociation events. Thus, we performed steered MD simulations to allow the systems to sample the whole dissociation or binding pathway. We used umbrella sampling to pull the Gem or CGem out of the LDL model with a harmonic potential of 1000 kJ/mol/nm^2. The collective variable we chose was the center of mass distance between the drug and LDL. The pulling rate was optimized to 0.0005 nm/ps to maintain the equilibrium as much as possible. We found that a faster pulling rate for CGem would perturb the system significantly by dragging one lipid molecule. The force constant used on the CGem was also found to be sufficient to restrain the Z position. Sampling windows were selected by a distance interval of 0.25 nm along the Z axis to ensure the overlap of the phase space between each adjacent window. Each window was sampled for 10 ns, and the last 5 ns were used for statistical analysis. The potential of mean force profiles was then calculated using the Gromacs package's weighted histogram analysis method (wham) algorithm.

DOI: 10.54254/2753-8818/73/2024.19379

3. Results and Discussions

3.1. Equilibration of the LDL Model

One criterion in our simulation pipeline is that the LDL model should be well-equilibrated prior to subsequent modeling of its interaction with drug molecules. In an NPT simulation, we observed the convergence of bulk quantities in the simulation to ensure the equilibration of the system. In Figure 4a, the temperature reached the target temperature of 310K quickly and remained stable over the remainder of the simulation. Similarly, the potential energy converged efficiently and remained stable within the 100 ns simulation period (Figure 4b). This indicates that the LDL system is well-relaxed in our equilibration period. Furthermore, we investigated the partial density of each component to ensure that the model was equilibrated on the atomic level. Figure 4c displays the distribution of each component along the Z-axis of the simulation box, with an equilibrated structure being imposed for better visualization. The partial overlap between water and the head group of POPC and LYPC indicates that the membrane was properly solvated by water molecules. Within the hydrophobic core, the symmetric distribution of GOTR, CHOE, and CHL further confirmed that the model is fully relaxed, resulting in a time-averaged area per lipid of 0.69 nm^2, similar to the reported results of the POPC membrane. Overall, the structure of the constructed LDL was reasonable and ready for subsequent modeling and simulations.

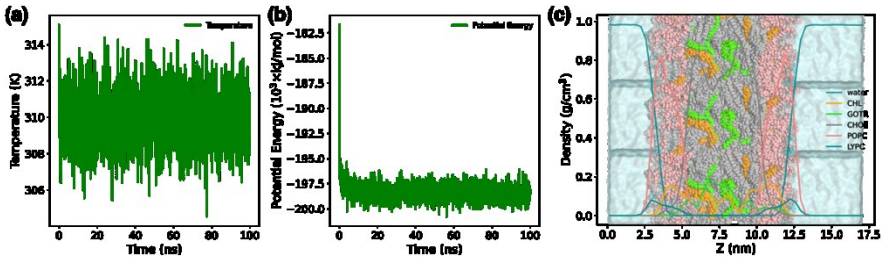


Figure 4. Equilibration of the LDL bilayer model. The convergence of temperature (a), and potential energy (b) of the simulation system. (c) The partial density of each component along the z coordinate acquired from the final 25 ns trajectory.

3.2. The Partition of Drugs to LDL

In physiological conditions, drugs after intravenous injection will encounter a complex chemical environment consisting of biomolecules (e.g., proteins, LDLs), ions, and cell entities. The exact emulation of such an environment is unfeasible due to the intricate compositions. Focusing on our hypothesis that cholesterol conjugation to hydrophilic chemotherapy drugs can leverage LDL to target cancer cells, we simplified the model by including only the LDL and drug of interest, neglecting the relatively trivial components in a physiological condition. The free Gem drug molecule serves as a control study for the CGem drug molecule.

To study the free interaction between Gem or CGem and the LDL model, we inserted the drug molecule into the water phase, respectively, to generate two independent simulations. The binding of drugs into the LDL can be approximated as the drug's leveraging an LDL in a physiological condition. First, we investigated the partial density of the drug molecules within the LDL model to determine the average depth of the drug's partition into the LDL. In Figure 5a, we show that CGem is located deeper with the LDL, possibly due to the hydrophobic interaction between the cholesterol tail of CGem with the hydrophobic core of LDL. In contrast, Gem, due to its hydrophilic nature, lies superficially on the lipid membrane with a large density overlap with the water phase.

DOI: 10.54254/2753-8818/73/2024.19379

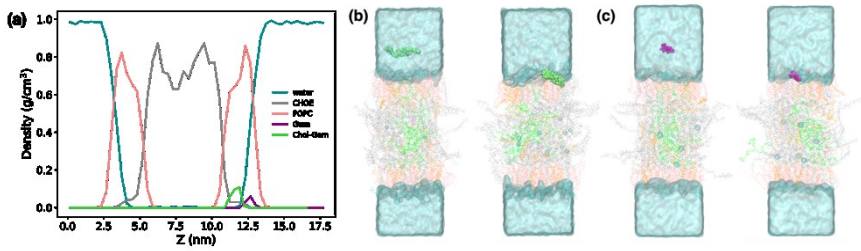


Figure 5. The binding of Gem and CGem to the LDL model. (a) The partial density profile of each drug against the major LDL model, including water, CHOE, and POPC. Initial position and final bound state of CGem (b) and Gem (c) in the LDL. The bulk water, cholesterol, CHOE, GOTR, POPC, and LYPC are shown in cyan, orange, gray, green, pink, and dark green, respectively. The CGem is shown in lemon green, and Gem is shown in purple.

In Figure 5b-c, we provide the initial and final bound positions of CGem and Gem. Each drug's initial position is positioned above 1 nm above the LDL model to prevent direct interactions, ensuring a spontaneous and random interaction between the drug and LDL. Consistent with Figure 5a, after a long equilibration and stabilization of the drug position, CGem shows a deeper insertion into the LDL model while Gem remains adjacent to the water phase. This further corroborates the findings that CGem can bind to LDL in a deeper position due to the hydrophobic interactions.

3.3. Binding Free Energy

The qualitative observation that CGem partitioned deeper into the LDL encouraged us to investigate the energies related to this partition behavior to quantitatively determine the binding strength between drugs and LDL. We hypothesized that CGem would encounter a higher free energy barrier during the dissociation process, starting from its binding configuration. In other words, the CGem is anticipated to experience a higher free energy decrease (i.e., stabilization) during the binding process compared with the unconjugated free Gem drug.

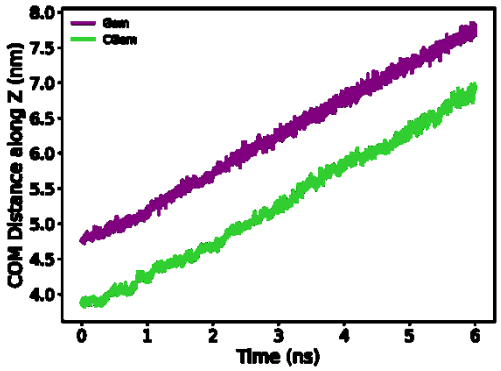


Figure 6. The COM distance between CGem or Gem and the LDL model. The simulation was conducted along a 6 ns period to progressively pull the drug out of the LDL model.

The enhanced sampling technique, umbrella sampling, was employed to improve the sampling in the low-probability (rare) events during the path. The reaction coordinate, which is a low-dimension projection of the degrees of freedom of the system, was the distance between the center of mass (COM) of the drug and the COM of LDL. The restraint was applied solely to the Z direction while keeping the X and Y dimensions unconstrained. To acquire the sampling windows for the umbrella sampling, steered MD simulations were conducted for both systems, and the progression of the Z distance between CGem and Gem is shown in Figure 6. We observe that the pulling force and rate we used resulted in a smooth

DOI: 10.54254/2753-8818/73/2024.19379

transition from a bound state to a dissociated state. From the pulling trajectories, we determined 17 sampling windows for each system to obtain the free energy of the dissociation process.

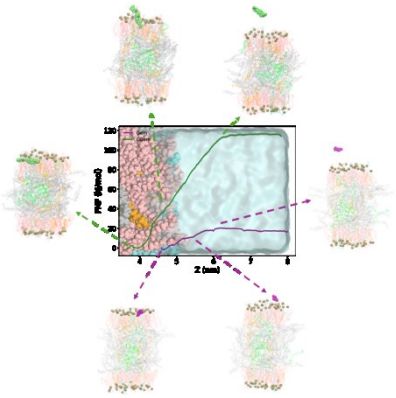


Figure 7. The PMF profiles of the dissociation of CGem and Gem from LDL. Three representative configurations during the sampling path are shown for each. The CGem and Gem are shown in lime green and magenta, respectively. The phosphorus atoms were shown in brown beads to indicate the upper and lower boundary of the LDL model.

In Figure 7, the free energy profiles indicate that CGem binds to LDL with a magnitude of higher energy gain compared with Gem. We identified a COM distance over 7 nm as the unbound state, and the associated free energy was averaged over quantities beyond that distance. On average, the CGem has a dissociation-free energy of 115.89 kJ/mol, while Gem has a dissociation-free energy of 17.23 kJ/mol. A free energy of 17.23 kJ/mol corresponds to 6.68 k_BT, which can be readily overcome in a physiological environment, leading to dissociation. In the reversible path, CGem would thus have a higher binding affinity than Gem with a magnitude higher free energy drop, implying that once the CGem binds to LDL in a biological condition, it would form a more stable adduct than the free drug Gem and that the probability of the dissociation of CGem from LDL would be significantly lower. The quantitative free energy comparison confirmed our hypothesis that the cholesterol conjugation to hydrophilic chemotherapy drugs can aid the drug to bind to LDL stably, which potentially promotes the subsequent targeting of the cholesterol-drug conjugate to cancer cells because of the circulation and targeting of LDL particles to cancer in the body.

4. Conclusions

The concept of designing cancer-targeting therapeutics has long been proposed, with the potential advantages of enhancing drug pharmacodynamics and treatment outcomes, as well as alleviating side effects. It has resulted in a wide exploration of drug modifications, nanocarriers, and targeting moieties. However, a number of the efforts introduce exogenous components, such as utilizing organic or inorganic nanoparticles or modifying agents with synthetic peptides, proteins, polymers, or chemicals, which may possess intrinsic immunogenicity and limited generalizability to different cancer types due to the specific targeting of cancer surface markers [45,46]. Exploiting endogenous cancer-targeting systems emerges as a new technology to improve the safety and generalizability of anti-cancer drugs. Among all the systems, LDL is an essential natural entity that targets a wide array of cancers via enhanced expression of LDL receptors on the cancer cell surface, holding outstanding potential as a natural vehicle for anti-cancer therapeutics.

In this contribution, we proposed a potential general prodrug design strategy—cholesterol conjugation to a chemotherapy drug—and confirmed its ability to employ LDL for drug delivery via all-atom MD simulations (Figure 1). The cholesterol-modified model drug (CGem) exhibits a deeper partition to the hydrophobic interior of the LDL model, whereas the free drug (Gem) is bound to the superficial hydrophilic layer. Further computation on the binding free energies revealed that CGem has

a magnitude higher binding affinity. The results confirmed our hypothesis that cholesterol conjugation to hydrophilic drugs can help the drugs bind to LDLs, which then subsequently promotes drug accumulation in cancer because of the LDL targeting. This simple cholesterol conjugation is anticipated to be generalizable to other small-molecule drug systems regardless of its hydrophobicity, under the premise that the chemical modification does not significantly hamper the efficacy of the drug itself.

In the future, the exploration of cholesterol conjugation should be explored experimentally, such as by quantifying the drug accumulation in the *ex vivo* LDL particles and in the *in vivo* tumor sites in mouse models. One caveat of the strategy would be the drug's release efficiency from the conjugates as it acts on tumor cells in its free form. Thus, the design of the linkage that ensures efficient release of the free drug in cancer cells should be considered, such as introducing enzyme-catalyzed cleavage linkers or pH-induced hydrolysis linkers. We anticipate that with the careful design of the complete prodrug, one can generate a wide array of potent cancer-targeting therapeutics that may improve the current cancer treatment regime and eventually contribute to human public health.

References

[1] Siegel, R. L., Miller, K. D., Wagle, N. S., & Jemal, A. (2023). Cancer statistics, 2023. *CA: A Cancer Journal for Clinicians*, *73*(1), 17–48. https://doi.org/10.3322/caac.21763

[2] Sung, H., Ferlay, J., Siegel, R. L., Laversanne, M., Soerjomataram, I., Jemal, A., & Bray, F. (2021). Global Cancer Statistics 2020: GLOBOCAN Estimates of Incidence and Mortality Worldwide for 36 Cancers in 185 Countries. *CA: A Cancer Journal for Clinicians*, *71*(3), 209–249. https://doi.org/10.3322/caac.21660

[3] Jenkins, R., Walker, J., & Roy, U. B. (2023). 2022 cancer statistics: Focus on lung cancer. *Future Oncology*, *73*(1). https://doi.org/10.2217/fon-2022-1214

[4] Kaur, R., Bhardwaj, A., & Gupta, S. (2023). Cancer treatment therapies: traditional to modern approaches to combat cancers. *Molecular Biology Reports*, *50*. https://doi.org/10.1007/s11033-023-08809-3

[5] Compton, C. (2020). Correction to: Cancer: The Enemy from Within. *Cancer: The Enemy from Within*, C1–C2. https://doi.org/10.1007/978-3-030-40651-6_13

[6] DeVita, V. T., & Chu, E. (2008). A History of Cancer Chemotherapy. *Cancer Research*, *68*(21), 8643–8653. https://doi.org/10.1158/0008-5472.can-07-6611

[7] Tobias, J., & Hochhauser, D. (2014). *Cancer and its Management Tobias/Cancer and its Management* (pp. 81–112). Chichester, Uk John Wiley & Sons, Ltd.

[8] Skeel, R. T., & Khleif, S. N. (2011). *Handbook of cancer chemotherapy* (p. 69). Lww.

[9] Ritter, J. M., Flower, R. J., Henderson, G., Yoon Kong Loke, MacEwan, D., Robinson, E., & Fullerton, J. (2023). *Rang & Dale's Pharmacology E-Book* (p. 690). Elsevier Health Sciences.

[10] Chidambaram, M., Manavalan, R., & Kathiresan, K. (2011). Nanotherapeutics to Overcome Conventional Cancer Chemotherapy Limitations. *Journal of Pharmacy & Pharmaceutical Sciences*, *14*(1), 67–77. https://doi.org/10.18433/J30C7D

[11] Olsen, M. M., Lefebvre, K. B., Brassil, K. J., & Oncology Nursing Society. (2019). *Chemotherapy and immunotherapy guidelines and recommendations for practice*. Oncology Nursing Society.

[12] Liu, T., Guo, C., Xu, S., Hu, G., & Wang, L. (2023). A Novel Strategy to Improve Tumor Targeting of Hydrophilic Drugs and Nanoparticles for Imaging Guided Synergetic Therapy. *Advanced Healthcare Materials*, *12*(26). https://doi.org/10.1002/adhm.202300883

[13] Dash, A., & Singh, S. (2023). *Pharmaceutics* (pp. 115–143). Elsevier.

[14] Busatto, S., Walker, S. A., Grayson, W., Pham, A., Tian, M., Nesto, N., Barklund, J., & Wolfram, J. (2020). Lipoprotein-based drug delivery. *Advanced Drug Delivery Reviews*, *159*, 377–390. https://doi.org/10.1016/j.addr.2020.08.003

[15] Murtola, T., Vuorela, T. A., Hyvönen, M. T., Marrink, S.-J., Karttunen, M., & Vattulainen, I. (2011). Low density lipoprotein: structure, dynamics, and interactions of apoB-100 with lipids. *Soft Matter*, *7*(18), 8135. https://doi.org/10.1039/c1sm05367a

[16] Sobot, D., Mura, S., Yesylevskyy, S. O., Dalbin, L., Cayre, F., Bort, G., Mougin, J., Desmaële, D., Lepetre-Mouelhi, S., Pieters, G., Andreiuk, B., Klymchenko, A. S., Paul, J.-L., Ramseyer, C., & Couvreur, P. (2017). Conjugation of squalene to gemcitabine as unique approach exploiting endogenous lipoproteins for drug delivery. *Nature Communications*, *8*(1), 15678. https://doi.org/10.1038/ncomms15678

[17] Yuan, Q., Lu, X., Guo, H., Sun, J., Yang, M., Liu, Q., & Tong, M. (2023). Low-density lipoprotein receptor promotes crosstalk between cell stemness and tumor immune microenvironment in breast cancer: a large data-based multi-omics study. *Journal of Translational Medicine*, *21*(1). https://doi.org/10.1186/s12967-023-04699-y

[18] Kazakova, E., Pavel Iamshchikov, Ирина Ларионова, & Kzhyshkowska, J. (2023). Macrophage scavenger receptors: Tumor support and tumor inhibition. *Frontiers in Oncology*, *12*. https://doi.org/10.3389/fonc.2022.1096897

[19] Upadhyay, R. K. (2018). Lipoproteins as drug delivery vehicles for cancer and tumor therapeutics. *Journal of Stem Cell Research & Therapeutics*, *4*(3). https://doi.org/10.15406/jsrt.2018.04.00115

[20] Harisa, G. I., & Alanazi, F. K. (2014). Low-density lipoprotein bio nanoparticles: From cholesterol transport to delivery of anti-cancer drugs. *Journal of the Saudi Pharmaceutical Society*, *22*(6), 504–515. https://doi.org/10.1016/j.jsps.2013.12.015

[21] Sarpietro, M. G., Micieli, D., Rocco, F., Ceruti, M., & Castelli, F. (2009). Conjugation of squalene to acyclovir improves the affinity for biomembrane models. *International Journal of Pharmaceutics*, *382*(1-2), 73–79. https://doi.org/10.1016/j.ijpharm.2009.08.012

[22] Saleh Ayed Alanazi, Gamaleldin Ibrahim Harisa, Badran, M. M., Haq, N., Awwad Abdoh Radwan, Kumar, A., Shakeel, F., & Fars Kaed Alanazi. (2020). Cholesterol-Conjugate as a New Strategy to Improve the Cytotoxic Effect of 5-Fluorouracil on Liver Cancer: Impact of Liposomal Composition. *Current Drug Delivery*, *17*(10), 898–910. https://doi.org/10.2174/1567201817666200211095452

[23] Radwan, A. A., & Alanazi, F. K. (2014). Targeting cancer using cholesterol conjugates. *Saudi Pharmaceutical Journal*, *22*(1), 3–16. https://doi.org/10.1016/j.jsps.2013.01.003

[24] Lv, X., Wang, P., Li, C., Cheng, S., Bi, Y., & Li, X. (2021). Zanamivir–Cholesterol Conjugate: A Long-Acting Neuraminidase Inhibitor with Potent Efficacy against Drug-Resistant Influenza Viruses. *Journal of Medicinal Chemistry*, *64*(23), 17403–17412. https://doi.org/10.1021/acs.jmedchem.1c01531

[25] Coppens, E., Didier Desmaële, Timothée Naret, Sébastien Garcia-Argote, Feuillastre, S., Pieters, G., Cailleau, C., Paul, J., Prost, B., Solgadi, A., Michel, J.-P., Noiray, M., Couvreur, P., & Mura, S. (2021). Gemcitabine lipid prodrug nanoparticles: Switching the lipid moiety and changing the fate in the bloodstream. *International Journal of Pharmaceutics*, *609*, 121076–121076. https://doi.org/10.1016/j.ijpharm.2021.121076

[26] Hollingsworth, S. A., & Dror, R. O. (2018). Molecular Dynamics Simulation for All. *Neuron*, *99*(6), 1129–1143. https://doi.org/10.1016/j.neuron.2018.08.011

[27] Grote, F., & Lyubartsev, A. P. (2020). Optimization of Slipids Force Field Parameters Describing Headgroups of Phospholipids. *The Journal of Physical Chemistry B*, *124*(40), 8784–8793. https://doi.org/10.1021/acs.jpcb.0c06386

[28] Ivanova, N., & Chamati, H. (2023). Physical properties of phospholipids at low temperatures through Slipid force field. *Journal of Physics*, *2436*(1), 012025–012025. https://doi.org/10.1088/1742-6596/2436/1/012025

[29] Wang, J., Wolf, R. M., Caldwell, J. W., Kollman, P. A., & Case, D. A. (2004). Development and testing of a general amber force field. *Journal of Computational Chemistry*, *25*(9), 1157–1174. https://doi.org/10.1002/jcc.20035

[30] Dickson, C. J., Rosso, L., Betz, R. M., Walker, R. C., & Gould, I. R. (2012). GAFFlipid: a General Amber Force Field for the accurate molecular dynamics simulation of phospholipid. *Soft Matter*, *8*(37), 9617. https://doi.org/10.1039/c2sm26007g

[31] Jójárt, B., & Martinek, T. A. (2007). Performance of the general amber force field in modeling aqueous POPC membrane bilayers. *Journal of Computational Chemistry*, *28*(12), 2051–2058. https://doi.org/10.1002/jcc.20748

[32] Mark, P., & Nilsson, L. (2001). Structure and Dynamics of the TIP3P, SPC, and SPC/E Water Models at 298 K. *The Journal of Physical Chemistry A*, *105*(43), 9954–9960. https://doi.org/10.1021/jp003020w

[33] Ke, Q., Gong, X., Liao, S., Duan, C., & Li, L. (2022). Effects of thermostats/barostats on physical properties of liquids by molecular dynamics simulations. *Journal of Molecular Liquids*, *365*, 120116. https://doi.org/10.1016/j.molliq.2022.120116

[34] Mazur, A. K. (1997). Common Molecular Dynamics Algorithms Revisited: Accuracy and Optimal Time Steps of Störmer–Leapfrog Integrators. *Journal of Computational Physics*, *136*(2), 354–365. https://doi.org/10.1006/jcph.1997.5740

[35] Huang, K., & García, A. E. (2014). Effects of truncating van der Waals interactions in lipid bilayer simulations. *The Journal of Chemical Physics*, *141*(10). https://doi.org/10.1063/1.4893965

[36] Essmann, U., Perera, L., Berkowitz, M. L., Darden, T., Lee, H., & Pedersen, L. G. (1995). A smooth particle mesh Ewald method. *The Journal of Chemical Physics*, *103*(19), 8577–8593. https://doi.org/10.1063/1.470117

[37] Simminent, A. C., & Brooks, B. R. (2021). A compression strategy for particle mesh Ewald theory. *The Journal of Chemical Physics*, *154*(5), 054112. https://doi.org/10.1063/5.0040966

[38] Noble, S., & Goa, K. L. (1997). Gemcitabine. *Drugs*, *54*(3), 447–472. https://doi.org/10.2165/00003495-199754030-00009

[39] Evans, D. A. (2014). History of the Harvard ChemDraw Project. *Angewandte Chemie International Edition*, *53*(42), 11140–11145. https://doi.org/10.1002/anie.201405820

[40] Csizmadia, P. (1999). MarvinSketch and MarvinView: Molecule Applets for the World Wide Web. *Proceedings of the 3rd International Electronic Conference on Synthetic Organic Chemistry*, 1–30. https://doi.org/10.3390/ecsoc-3-01775

[41] Luciano Porto Kagami, Wilter, A., Diaz, A., & Wim Vranken. (2023). The ACPYPE web server for small-molecule MD topology generation. *Bioinformatics*, *39*(6). https://doi.org/10.1093/bioinformatics/btad350

[42] Jakalian, A., Jack, D. B., & Bayly, C. I. (2002). Fast, efficient generation of high-quality atomic charges. AM1-BCC model: II. Parameterization and validation. *Journal of Computational Chemistry*, *23*(16), 1623–1641. https://doi.org/10.1002/jcc.10128

[43] Sacks, F. M., & Campos, H. (2003). Low-Density Lipoprotein Size and Cardiovascular Disease: A Reappraisal. *The Journal of Clinical Endocrinology & Metabolism*, *88*(10), 4525–4532. https://doi.org/10.1210/jc.2003-030636

[44] Martínez, L., Andrade, R., Birgin, E. G., & Martínez, J. M. (2009). PACKMOL: A package for building initial configurations for molecular dynamics simulations. *Journal of Computational Chemistry*, *30*(13), 2157–2164. https://doi.org/10.1002/jcc.21224

[45] Ding, L., Agrawal, P., Singh, S. K., Chhonker, Y. S., Sun, J., & Murry, D. J. (2024). Polymer-Based Drug Delivery Systems for Cancer Therapeutics. *Polymers*, *16*(6), 843. https://doi.org/10.3390/polym16060843

[46] Hua, S., de Matos, M. B. C., Metselaar, J. M., & Storm, G. (2018). Current Trends and Challenges in the Clinical Translation of Nanoparticulate Nanomedicines: Pathways for Translational Development and Commercialization. *Frontiers in Pharmacology*, *9*. https://doi.org/10.3389/fphar.2018.00790